Seismic Behaviour of RC Building Frame Considering Soil–Structure Interaction Effects

Nishant Sharma, Kaustubh Dasgupta, and Arindam Dey

Abstract Reinforced Concrete (RC) frame buildings constitute a large fraction of the urban building stock in India. During past earthquakes, a number of these buildings have been observed to suffer extensive damages. Although conventional code-prescribed seismic design methodology does not account for consideration of soil–structure interaction, the presence of soil can cause a significant change in the seismic behaviour of the buildings. The present article investigates the seismic behaviour of an RC building frame under the influence of nonlinear Soil–Structure Interaction (SSI). Finite element analysis of a five-storeyed building frame is carried out under applied ground motions to simulate the possible effects of earthquake shaking. Analysis of various response entities reveals the mechanisms by which the influence of SSI affects the structural behaviour. Moreover, the analysis demonstrates crucial aspects of the nonlinear behaviour and energy dissipation characteristics of the building frame under the influence of SSI. The study shows that seismic soil–structure interaction cannot be ignored, contrary to the present state of practice and guidelines of the design codes of various countries.

Keywords Soil–structure interaction · Frame building · Ground motion · Viscous boundaries · Nonlinear behaviour · Time history analysis

N. Sharma · K. Dasgupta (✉) · A. Dey
Department of Civil Engineering, Indian Institute of Technology Guwahati, Guwahati 781039, India
e-mail: kd@iitg.ac.in

N. Sharma
e-mail: nsharmanishant@gmail.com

A. Dey
e-mail: arindamdeyiitg16@gmail.com

S. Dutta et al. (eds.), *Advances in Structural Vibration*, Lecture Notes in Mechanical Engineering, https://doi.org/10.1007/978-981-15-5862-7_14

1 Introduction

Effect of seismic soil–structure interaction on the behaviour of the structure has been in debate for decades and the present state of practice is to ignore the effect of SSI for the seismic analysis and design of building structures. However, for a flexible foundation soil system, it is imperative that the interaction mechanism would play a role in the behaviour of the structure in the event of an earthquake. Also, very few past studies have simultaneously considered coupling of structural and soil nonlinearities in SSI problems. Therefore, behaviour of the structure considering nonlinear soil–structure interaction has not been investigated in detail. The present article attempts to investigate and understand the non-linear behaviour of the structure considering SSI effects by modelling the soil as a continuum along with the structure in the finite element based software framework, OpenSEES [1]. The structure chosen is modelled with various soil conditions and subjected to earthquake excitation using a ground motion record. The present article aims to understand how the non-linear behaviour of an RC building frame is modified with the inclusion of SSI effects.

2 Modelling

Two-dimensional modelling of the structure, foundation-soil system has been carried out in OpenSEES. The modelled SSI system along with the adopted mesh is shown in Fig. 1, and the modelling aspects are discussed in the following subsections.

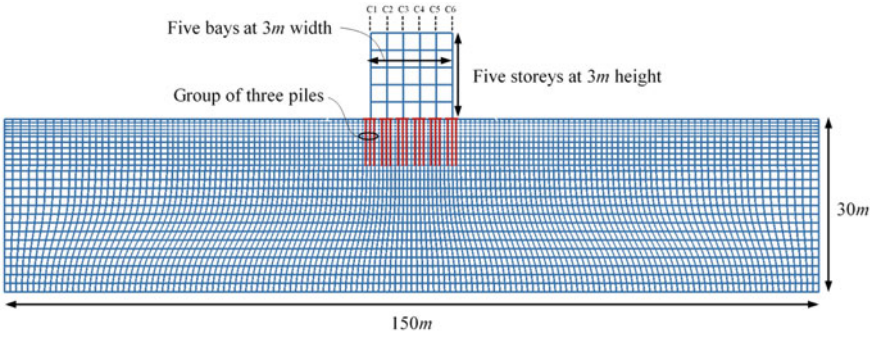

Fig. 1 SSI system and meshing adopted

Table 1 Details of reinforced concrete frame sections

Member	Size (mm^2)	Main r/f	Shear r/f
Beam	250 × 400	4@20 mm φ (+)	2 legged 8 mm@ 100[a]
		4@20 mm φ (−)	
Column	400 × 400	8@16 mm φ	3 legged 8 mm@ 75*; @ 200**
		Uniformly distributed	

[a]Uniform spacing of stirrup in millimeter (mm); *Spacing of stirrup near ends of the member in *mm*; **Spacing of stirrup elsewhere in member in millimeter (mm); (+) Tension reinforcement; (−) Compression reinforcement; $\varphi = dia$

2.1 Structural System

The structural system considered in the present study is a five-storied RC building frame with five bays. The uniform storey height and bay width are considered as 3 m, respectively. The structure is located on a soft soil site in Seismic Zone V as per the Indian seismic design code IS 1893: Part I [2]. For the purpose of design and analysis of the structure, relevant Indian standards have been referred [2–5]. The sectional details of the beams and the columns are shown in Table 1. Grade of concrete and reinforcing steel used are considered as M25 and Fe415, respectively. Various column locations have been marked as C1-C6 (Fig. 1). C1 and C6 are the exterior most columns, C2 and C5 are intermediate columns, and C3 and C4 are innermost columns.

2.2 Foundation Soil System

Rectangular sandy soil domain of length 10 times the structural base width (10 × 15 m = 150 m) is considered (Fig. 1). Bedrock is assumed to be at a depth of 30 m from the surface of the ground. Four-node quadrilateral elements, with bilinear isoparametric formulation, are used to model the soil as a continuum. A non-uniform meshing is adopted to appropriately capture the soil behaviour in the region of interest. In total, 3822 nodes and 3650 elements are used for representing the soil domain. The size of the smallest element used is 0.375 m.

Pile foundation is used for supporting the structure on the soil medium. The lateral force estimation and design of pile group have been done using IS 2911: Part I/Sec I [6] and other relevant Indian standards. Since significant nonlinearity is not expected in the pile groups, the pile elements are assigned linear elastic sectional properties. The piles are connected to the soil elements using zero-length rigid link member and interface nonlinearity has not been considered in the analysis. The pile groups are

Table 2 Details of soil properties and pile foundation

Soil type	ρ (t/m^3)	φ	ν	e	G_r (kPa)	Dia (m)	Length (m)	n
Soft Soil (SS)	1.7	29	0.33	0.85	5.5×10^4	0.5	8.0	3
Med Soil (MS)	1.9	33	0.33	0.70	7.5×10^4	0.5	7.0	3
Med Dense Soil (MDS)	2.0	37	0.35	0.55	1.0×10^5	0.5	6.0	3
Dense Soil (DS)	2.1	40	0.35	0.45	1.3×10^5	0.5	5.0	3

ρ = Density; φ = Friction angle; ν = Poisson's ratio; G_r is reference low strain shear modulus measured at 80 kPa reference pressure, n = number of piles in a group

connected to each other using grade beams of size 0.4 m × 0.4 m. In the present study, four different types of soil have been considered and for each soil condition, the pile groups have been designed. In practice, it is common to keep the diameter of the piles as the same for various locations and to adjust the length of the piles for obtaining the appropriate design capacity of the pile foundation. Therefore, in the present study, the pile groups for different soil conditions have been designed keeping the diameter as 0.5 m and appropriate lengths. Table 2 shows the basic soil properties considered and the details of pile groups designed.

2.3 Material Properties

PressureDependMultiYield material has been used to simulate the nonlinear behaviour of the soil. The plastic behaviour in this material model follows the Drucker–Prager yield surfaces (nested yield surface) criteria. Stress–strain data for confined and unconfined concrete are obtained using the relationships prescribed by Chang and Mander [7] and they are shown in Fig. 2a. The stress–strain relationship used to model the reinforcing steel [8] is shown in Fig. 2b. The stress–strain values are assigned to the fiber section for modelling the beam and the column sections.

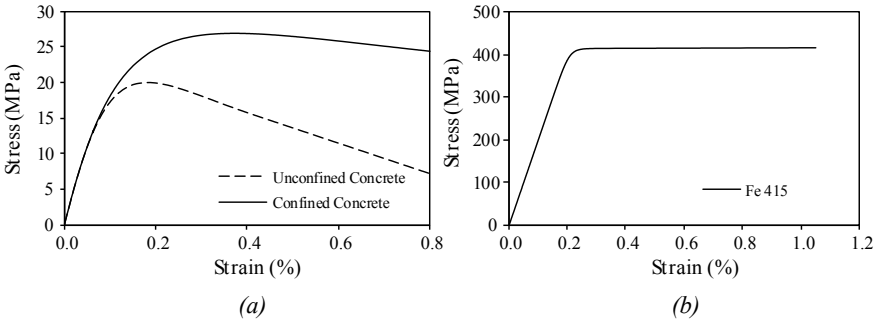

Fig. 2 Stress–strain relationship for **a** concrete **b** rebar steel

2.4 Plastic Hinge

The nonlinearity in the building frame is considered in the form of lumped plastic hinges that develop over a length at the ends of the member. The length of the plastic hinge for the members is obtained using the relationship shown in Eq. (1) proposed by Paulay and Priestley [9].

$$l_p = 0.08l + 0.022d_b \tag{1}$$

where l_p is the length of plastic hinge, l is the distance between the points of contraflexure and d_b is the diameter of the longitudinal bar used. The assignment of plastic hinge length ensures that the nonlinearity developed in the building frame members is localized at the end regions.

2.5 Soil Domain Boundaries

For SSI studies, modelling of the boundaries is very important to simulate the effect of radiation damping and the application of excitation input. Also, proper modelling of the boundaries allow the truncation of the soil domain to a finite extent. In the present study, the vertical and horizontal boundaries have been modelled using Lysmer–Kuhlemeyer viscous dashpots [10] to arrest the waves at the boundary in the transverse and longitudinal directions and to prevent the same from reflecting back into the soil medium after being incident at the far-off boundaries. The ground motion input, for to the SSI cases, is applied in the form of equivalent nodal forces using the procedure outlined in [11]. For the structure supported on rock (R), it is appropriate to restrain the translational and the rotational degrees of freedom at the column bases to simulate the characteristics of rocky medium (R).

3 Rayleigh Damping

The presence of nonlinearity in the soil produces high-frequency spurious oscillations, due to underdamped modes, in the numerical solution of the SSI system. To overcome the issue, the HHT-α method for time step integration [12] may be used. For cases wherein the HHT-α method is ineffective for removal of the spurious oscillations, incorporation of a small amount of Rayleigh damping is useful. Therefore, in the present study, Rayleigh damping has been considered. It is assumed that all the contributing modes are having approximately the same damping ratio of 5%. For the fixed base analysis, the frequencies of the various modes of the structure can be estimated using the conventional eigenvalue analysis. However, for the SSI system,

Table 3 Rayleigh damping coefficients

Soil type	Avg. v_s (m/s)	ω_1 (rad/s)	ω_2 (rad/s)	a_0	a_1
Soft Soil (SS)	190	29.85	49.74	1.86	0.001
Med Soil (MS)	220	34.56	57.60	2.16	0.001
Med Dense Soil(MDS)	250	39.27	65.45	2.45	0.001
Dense Soil (DS)	280	48.93	73.30	2.75	0.001

the conventional eigenvalue analysis cannot be applied. Hence, the theoretical relationship mentioned in [13] is used. The frequencies corresponding to the first and the second mode are chosen for the estimation of Rayleigh damping coefficients using the relationships mentioned in [14]. Based on the damping ratios and the frequency of the modes, the coefficients are estimated to form the damping matrix. Table 3 shows the details of the frequencies and Rayleigh damping coefficients, corresponding to the structure and the soil used for the formation of the damping matrix.

4 Gravity and Time History Analyses

To conduct a dynamic analysis of the structure–soil system, it is a prerequisite to carry out static gravity analysis in a staged manner [15]. Moreover, before conducting a full-fledged analysis of the soil–structure system, it is necessary to ensure accurate incorporation of boundary conditions. For this, a linear elastic soil model (without structure) with sine wavelet as input has been analyzed and the model is validated for the response in the centre of the soil domain as shown in Fig. 3a. Figure 3b shows the ground motion selected for performing time history analysis to study the soil–structure interaction effects after performing gravity analysis. To reduce the computational time, only the significant duration of the ground motion has been

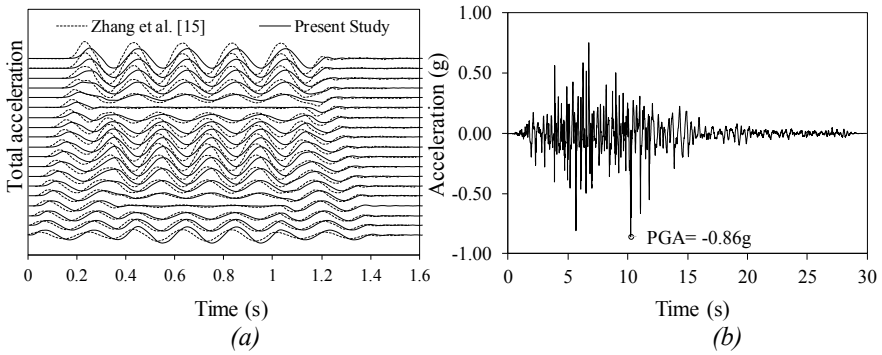

Fig. 3 **a** Validation of the SSI model **b** ground motion used for time history analysis

used in conducting the time history analysis. The significant duration is the time duration of the ground motion during which the Arias Intensity is above 5% but not more than 95% of the total Arias Intensity developed over the duration of the entire ground motion.

5 Results and Discussion

5.1 Time History Response

Figure 4a and 4b shows the comparison of roof displacement response and shear developed at the base of first storey columns, respectively. It can be observed that the response of the structure supported on Soft Soil (SS) lags as compared to the structural response with other types of supporting soil (MS, MDS and DS) or rocky condition (R). This is due to the fact that in soft soil the propagation of the shear waves is slower due to its density being less than other stiffer soils or rocky medium. The peak roof displacement is highest for Medium Soil (MS) and for other soil conditions (SS, MDS and DS) the value is slightly lower, and it is lowest for structure supported on rock (R). For the structure supported on rock, a larger number of well-defined peaks and crests are visible in the response as compared to those for the structure supported on soils (SS, MS, MDS and DS). Except for the absolute maximum value of the response, most peaks are greater in magnitude for the structure on rock (R). It can be observed that many small peaks, observed for the structure on rock (R), are subdued for the structure supported on soil (SS, MS, MDS and DS). Moreover, the peaks forming in the duration of 4–8 s (as seen for rocky site) result in the build up of a larger peak for the structure supported on soil. This leads to the peak response

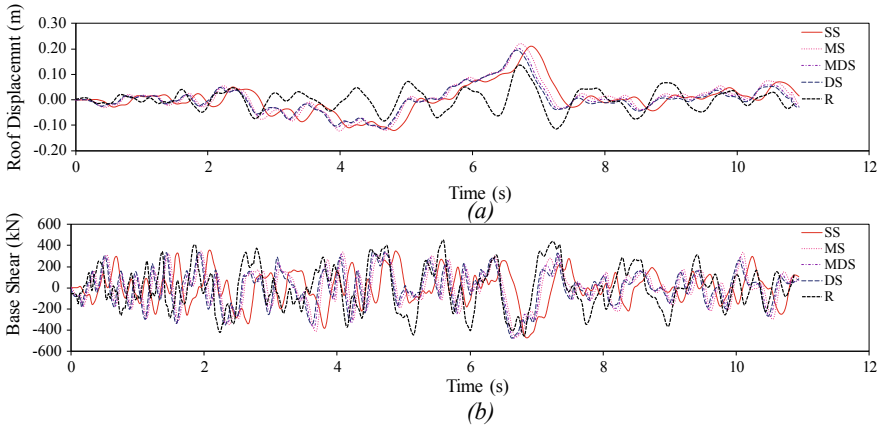

Fig. 4 Comparison of time histories for **a** roof displacement **b** base shear

in the structure supported on soil (SS, MS, MDS and DS) to be greater than that of the structure supported on rock (R).

The observed phenomenon can be explained by relating to the nonlinear behaviour exhibited by the soil. When a wave propagates towards the structure, it forces the structure to get displaced in one direction. A wave having sufficient energy remaining, after undergoing radiation damping and hysteretic damping, tends to displace the structure in a particular direction. If the wave does not have sufficient energy remaining after the dissipation, then, the structure is unable to undergo significant displacement and a potential peak is unable to develop. As observed in the case of rocky strata, for example, in Fig. 4a, it can be seen that the wave after 4.5 s pushes the structure supported on rock as well as soil in the direction of positive displacement. Once the peak is attained, the wave tries to push the structure back in the negative displacement direction. The mentioned phenomenon is observed for structure supported on rock (R). However, for structure supported on soil (SS, MS, MDS and DS), sufficient energy is not available after hysteretic damping and radiation damping so as to displace the structure in the negative direction (as observed in the case of the structure supported on rock). This inhibits the formation of a peak in the negative direction. At the same instant, another wave strikes and tries to displace the structure in the positive direction and leads to the development of a low frequency and high amplitude wave, as can be seen from Fig. 4a, for the structure supported on soil. The inability of the seismic waves to displace the structure in the negative direction causes the structure to displace further in the positive direction. A similar process is repeated for the next wave as well resulting in an overall buildup of the displacement in the positive direction for the structure supported on soil. This causes the displacement of the structure supported on soil to be higher than that of the structure supported on rock even though the latter is subjected to higher energy from the ground motion. Similar observations are made for base shear (Fig. 4b), and can be explained likewise. From Fig. 4a and 4b, it can also be seen that as the stiffness of the soil is reducing from DS to MS, the peak displacement and base shear tend to increase. However, on further reducing the stiffness of the soil from MS to SS, a slight drop in the peak values can be observed. This can be due to the fact that the reduction in the stiffness of the soil from MS to SS allows for higher nonlinear hysteretic behaviour in soil, leading to higher energy dissipation and reduction in the energy content of the waves being transmitted to the structure. Hence, reducing the peak displacements/base shear for the structure supported on SS compared to that of the structure supported by MS.

Figure 5a and 5b presents the maximum floor level accelerations ($a_{\max}$) and root mean square acceleration (a_{rms}), respectively, in the structure for different soil conditions. It can be seen that $a_{\max}$ for the structure on rock is highest for all storey (floor) levels. For a structure supported on soft soil (SS), the value is the least for most of the storey levels. As the stiffness of the soil increases from SS to DS, the profile of $a_{\max}$ for various storey levels approaches that of the structure supported on rock (R). For structures supported on SS and MS, $a_{\max}$ is highest at the topmost storey level. However, for structure supported on MDS, DS and R, $a_{\max}$ increases till the second storey level thereafter it reduces till the fourth storey and again increases at

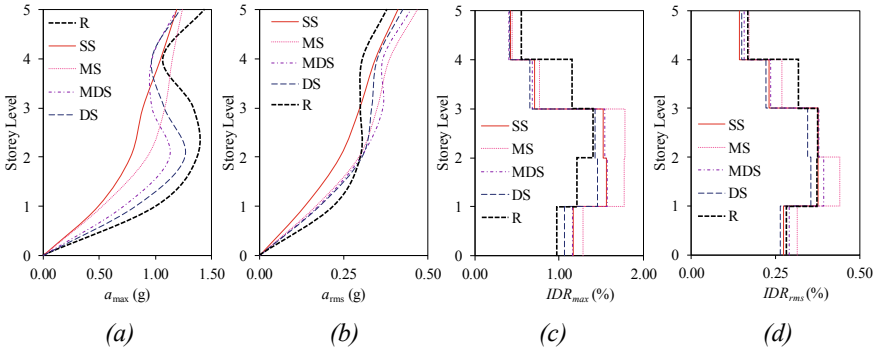

Fig. 5 Comparison of storey level peak and root mean square responses. **a** acce1eration a_{max}, **b** acceleration a_{rms}, **c** interstorey drift ratio IDR_{maz}, **d** interstorey drift ratio IDR_{rms}

the fifth storey level. To get an idea of the magnitude of the floor level accelerations developed over the entire duration of the time history, root mean square acceleration (a_{rms}) is obtained and plotted at various storey levels in Fig. 5b. It can be seen that for SS and MS, higher storey levels develop greater accelerations. As the stiffness of the soil is increased from MS to R, there is a reduction in a_{rms} at higher storey levels but the same increases at the lower storey levels. The average a_{rms} are obtained by averaging the a_{rms} values for all the storey levels. It has been observed that the structures supported on MS, MDS and DS experience 11%, 10% and 5% more acceleration whereas for the structure supported on SS the average a_{rms} experienced is 6% lesser than that compared to the structure supported on rock.

The difference in the trend for softer and stiffer soils may be due to the fact that the structure supported on SS and MS deform primarily according to the fundamental mode shape as the high-frequency oscillations are filtered out in the presence of soft or loose soil. On being excited by the fundamental mode, it is imperative that the higher storey levels develop larger accelerations. For structure supported on MDS, DS and R, apart from the fundamental mode shape, higher modes may also get excited during the deformations. The excitation of the higher modes allows for the development of larger accelerations in the intermediate storey levels, leading to the trends as observed for a_{max} and a_{rms}. The two entities (a_{max} and a_{rms}) provide a qualitative estimate of the forces being experienced by the structural frame for different soil conditions as inertial forces are directly proportional to the acceleration. Figure 5c and 5d shows the maximum and root mean square Interstorey Drift Ratios (IDR_{max} and IDR_{rms}), respectively. For lower storey levels, the structure supported on soil is subjected to greater IDR_{max}. However, for higher storey levels storey levels, it is the structure supported on rock, which is subjected to higher IDR_{max}. It can also be seen that as the stiffness of the soil gets reduced from type R to type MS, IDR_{max} tends to increase for the lower storey levels and get reduced for the higher storey levels. On further reduction of the soil stiffness, a reduction in IDR_{max} for lower storey levels is observed. Figure 5d shows the comparison of IDR_{rms} for various storey levels. It

provides an estimate of the average interstorey drift ratio experienced by the structure over the entire duration of the time history. A drastic change in the IDR at a storey level indicates the occurrence of large deformations at that level. For the structure supported on soil, a sharp drop in the IDR_{max} and IDR_{rms} values can be seen at the level of the third storey. However, for the structure supported on rock, a drop is seen at the third storey level and a sharper drop is seen at the fourth storey level. Large storey deformations can occur if the column members at that storey level yield significantly. Further investigation of nonlinear structural behaviour is discussed in the following subsection.

5.2 *Structural Nonlinearity*

The nonlinearity in the structure is defined in terms of the plastic hinge locations and to study the nonlinear behaviour of the structure, the mobilized moment–curvature (M-φ) relationships are obtained. Since it is not possible to discuss the M-φ response at all the column sections, only some noteworthy results are discussed herein. Figure 6a and 6b shows the M-φ response at the column locations C1 and C6 at the base of the first storey, respectively. Similarly, Fig. 6c and 6d shows the M-φ response at the column locations C1 and C6 at the top of the third storey, respectively. It can be observed that the columns of the building frame supported on soil show unsymmetrical behaviour as compared to that of the structure supported on rock (R),

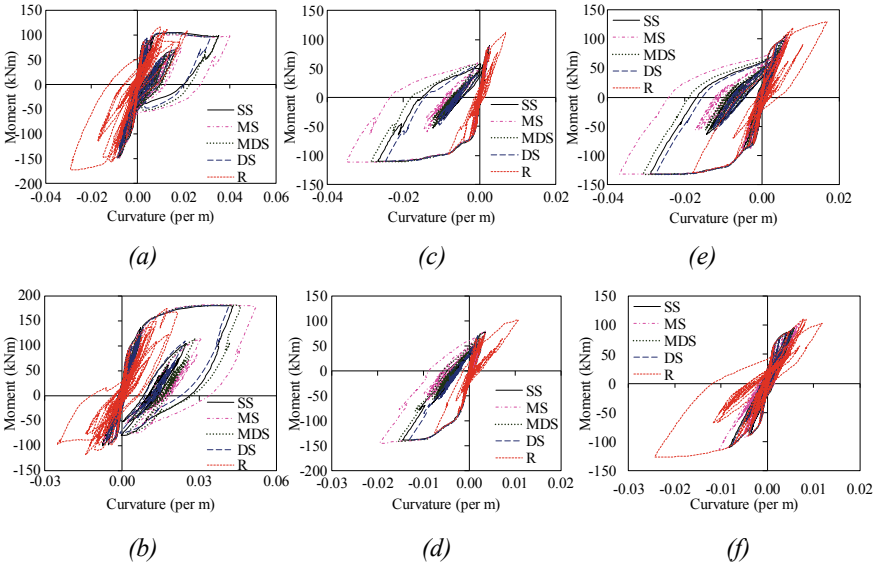

Fig. 6 Comparison of moment-curvature response at base of first storey columns. **a** C1, **b** C6 third storey columns **c** C1, **d** C6 **e** third storey column C4 **f** fourth storey column C2

i.e. large curvature in one particular direction and small curvature along the other direction. This can be attributed to the modification of the structural response due to interaction effects as observed in Fig. 4. The development of a low-frequency, high-amplitude wave pushes the structure in one particular direction and causes the development of moments and curvatures in that direction. This leads to such unsymmetrical M-φ behaviour, which is not observed in the columns of the building frame supported on rock (R). It can also be observed that among all the soil conditions, it is the columns of the structure supported on medium soil (MS) that develop the largest curvature and hence its sections yield more as compared to the columns of the building frame supported on other rock or soil conditions. This is due to the high acceleration values developed in the structure supported on the medium soil as discussed for Fig. 5a and 5b. Higher accelerations induce greater inertial forces within the structure and consequently develop larger displacements and curvatures. It is to be noted that the curvatures and moments developed for the third storey columns are in the opposite direction to those developed in the first storey columns, indicating a change in the curvature of the deformed shape. Such behaviour is expected in a frame wherein the redundancy provided by various columns and beams does not allow the frame to deform like a cantilever. It can be seen that although both the columns are under similar gravity loading condition, the mobilized moment capacity of columns at C6 is higher than that of the columns at C1. This is because, on being subjected to the ground motion, the structure displaces more in the positive direction over the entire duration due to which the exterior columns at C6 are subjected to additional axial compressive forces while the column at C1 is subjected to a reduction in compressive force at the same time. The additional compressive forces prevent the fibres of the section to undergo failure and hence are responsible for the increased moment capacity of the columns at C6.

Figure 6e and 6f represents the nonlinear behaviour at the top of the third storey and the fourth storey columns, respectively. It can be seen that for the structure supported on soil (SS, MS, MDS and DS), the third storey columns show significant yielding. For the structure supported on rock (R) besides the third storey columns, the fourth storey columns also yield significantly. To confirm the observed trend, the energy dissipated by the frame members is estimated from the hysteresis loops exhibited by the M-φ relationships of the various members.

Figure 7a shows the comparison of the storey-wise energy dissipated by the structure. Figure 7b and 7c shows the contribution of the energy dissipated by the beams and columns, respectively. Figure 7d shows the gross total energy dissipated by the structure for the different soil conditions. From the figures, it can be observed that the energy dissipated by structure on MS is the maximum followed by the structures supported on R, MDS, SS and DS types of soil. Storey wise, it is the first storey which undergoes the highest nonlinearity followed by the third storey and subsequently the other storey levels. It can be seen that the first and the third storey columns undergo significant nonlinearity for the structure supported on soil. For the structure supported on rock, the second, third and the fourth storey columns exhibit a similar extent of nonlinearity. This is in agreement with the observations in Fig. 5e and 5f. In addition, for the structure supported on rock, significant yielding of columns occurs for

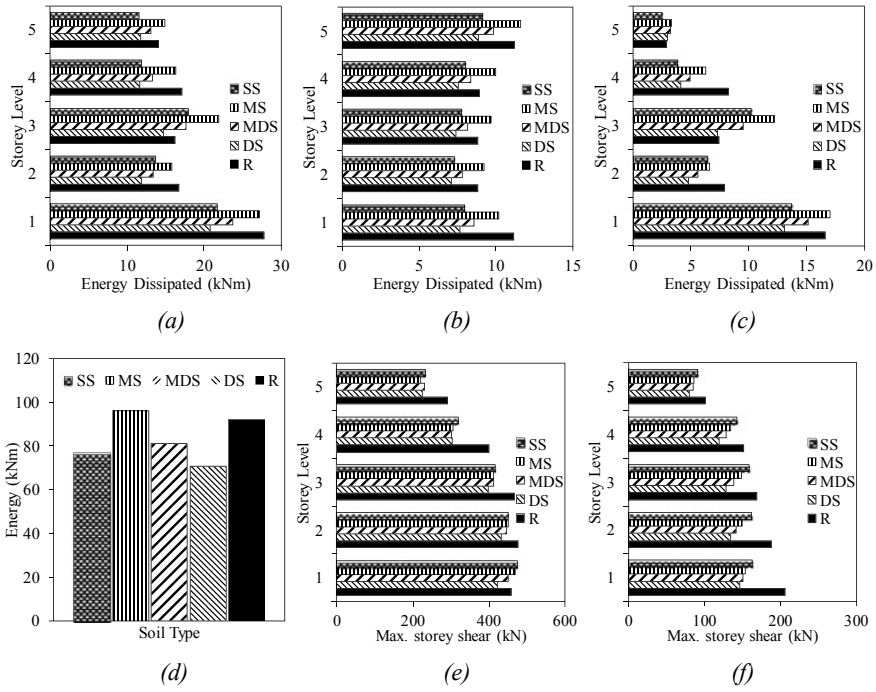

Fig. 7 Comparison of **a** storey-wise total energy dissipation **b** storey-wise energy dissipation in beams **c** storey-wise energy dissipation in columns **d** gross total energy dissipated **e** maximum storey shear **f** RMS storey shear

the second, third and fourth storey levels. However, for the structure supported on soil, the yielding of columns of the second and the fourth storey levels are relatively less than the yielding of columns in the third storey. For the structure supported on rock, the fourth storey is susceptible to greater damage due to the reduced moment capacity of the columns, as the gravity load is reduced at higher storey levels. Thus, for the rocky condition, although the second, third and fourth storey levels dissipate similar amounts of energy, still, the columns at the fourth storey undergo larger rotations/curvatures as seen from Fig. 5f. Also, due to the large rotations developed at the fourth storey level, a sharp drop in the interstorey drift is observed for the structure supported by rock. For the structure supported on soil, a sharp drop in the interstorey drift ratio is observed at the third storey level due to the columns undergoing larger nonlinear deformations at that storey (Fig. 5c and d). Hence, the failure of the columns get shifted to the lower storey levels when the structure is supported on soil or vice versa. This can be understood with the help of Fig. 7d and e, which shows the storey-wise developed maximum and root mean square shear forces, respectively.

From the figures, it can be seen that for the structure supported by rock, shear developed in the fourth storey is comparable to the shear developed in the third storey of the structure supported by soil. This leads to the development of higher nonlinearity

at the higher storey levels for the structure supported on rock. The observation can be related to the sharp increase in the maximum acceleration developed at the fifth storey for the structure supported on rock (R). The corresponding induced inertial forces developed at the fifth storey may have been enough to cause the failure at the fourth storey level in the structure supported by rock (R). For the structure supported on soil, the inertial forces from the fifth storey may not have been sufficient to develop failure at the fourth storey columns. However, the combined inertial forces from the fourth and the fifth storey levels may have caused significant yielding in the columns at the third storey level, leading to the development of greater interstorey drift and curvature in the columns at that level. For beam members, it can be seen that all the storey levels develop comparable levels of nonlinearity in their sections.

6 Conclusions

From the present study, it can be concluded that soil–structure interaction can significantly modify the structural response and failure patterns. The study shows that the belief of soil flexibility not being detrimental rather beneficial has been found to be contradicted. It is possible that particular soil conditions could produce situations that may cause greater damage to the structure supported on soil than that supported on rock. Nonlinear soil–structure interaction has been found to modify the structural response, giving rise to low-frequency, high-amplitude excitations, which could develop larger forces at particular instants of time. This may be sufficient to push the structure towards failure especially at specific storey levels of the structure. The concentrated failure of the columns at a particular storey level may lead to the collapse of the structure. Hence, it is inferred that ignoring SSI may prove to be detrimental in certain cases and it would be wise to assess the problem on a case-by-case basis without generalizing the problem of soil–structure interaction as a whole.

References

1. Mazzoni S, McKenna F, Scott MH, Fenves GL (2006) OpenSEES command language manual. Pacific Earthquake Engineering Research (PEER) Center, USA
2. IS 1893: Part I (2016) Indian standard, criteria for earthquake resistant design of structures. Bureau of Indian Standards, New Delhi, India
3. IS 875: Part 2 (1987) Indian standard, code of practice for design loads (other than earthquake) for building and structures: Imposed loads. Bureau of Indian Standards, New Delhi, India
4. IS 456 (2000) Indian standard, plain and reinforced concrete-code of practice. Bureau of Indian Standards, New Delhi, India
5. IS 13920 (2016) Indian standard, Ductile detailing of reinforced concrete structures subjected to seismic forces-code of practice. Bureau of Indian Standards, New Delhi, India
6. IS 2911: Part I/Sec 1 (1979) Indian standard, code of practice for design and construction of pile foundations. Bureau of Indian Standards, New Delhi, India

7. Chang G, Mander J (1994) Seismic energy based fatigue damage analysis of bridge columns: Part I—Evaluation of seismic capacity. NCEER Technical Report 94-0006
8. Filippou FC, Popov EP, Bertero VV (1983) Effects of bond deterioration on hysteretic behavior of reinforced concrete joints. Report EERC 83-19. Earthquake Engineering Research Center, University of California, Berkeley, USA
9. Paulay T, Priestley MJN (1992) Seismic design of reinforced concrete and masonry buildings. Wiley, USA
10. Lysmer J, Kuhlemeyer RL (1969) Finite dynamic model for infinite media. J Eng Mech Div 95(EM4):859–877
11. Joyner WB (1975) Method for calculating nonlinear seismic response in 2-dimensions. B Seismol Soc Am 65(5):1337–1357
12. Hilber HM, Hughes TJ, Taylor RL (1977) Improved numerical dissipation for time integration algorithms in structural dynamics. Earthq Eng Struct D 5(3):283–292
13. Kramer SL (1996) Geotechnical earthquake engineering. Prentice Hall, USA
14. Chopra AK (1995) Dynamics of structures-theory and applications to earthquake engineering. Pearson Education Inc., India
15. Zhang Y, Yang Z, Bielak J, Conte JP, Elgamal A (2003) Treatment of seismic input and boundary conditions in nonlinear seismic analysis of a bridge ground system. In: 16th ASCE engineering mechanics conference, University of Washington, Seattle, USA, 16–18 July 2003